

# On Computations for Thermal Radiation in MHD Channel Flow with Heat and Mass Transfer

T. Hayat<sup>1,2</sup>, M. Awais<sup>3\*</sup>, A. Alsaedi<sup>2</sup>, Ambreen Safdar<sup>1</sup>

**1** Department of Mathematics, Quaid-I-Azam University, Islamabad, Pakistan, **2** Department of Mathematics, King Abdulaziz University, Jeddah, Saudi Arabia, **3** Department of Mathematics, COMSATS Institute of Information Technology, Attock, Pakistan

## Abstract

This study examines the simultaneous effects of heat and mass transfer on the three-dimensional boundary layer flow of viscous fluid between two infinite parallel plates. Magnetohydrodynamic (MHD) and thermal radiation effects are present. The governing problems are first modeled and then solved by homotopy analysis method (HAM). Influence of several embedded parameters on the velocity, concentration and temperature fields are described.

**Citation:** Hayat T, Awais M, Alsaedi A, Safdar A (2014) On Computations for Thermal Radiation in MHD Channel Flow with Heat and Mass Transfer. PLoS ONE 9(1): e86695. doi:10.1371/journal.pone.0086695

**Editor:** Yinping Zhang, Tsinghua University, China

**Received:** September 18, 2013; **Accepted:** December 12, 2013; **Published:** January 30, 2014

**Copyright:** © 2014 Hayat et al. This is an open-access article distributed under the terms of the Creative Commons Attribution License, which permits unrestricted use, distribution, and reproduction in any medium, provided the original author and source are credited.

**Funding:** The research of Dr. Alsaedi was partially supported by Deanship of Scientific Research (DSR), King Abdulaziz University, Jeddah, Saudi Arabia. No addition external funding was received for this study. The funders had no role in study design, data collection and analysis, decision to publish, or preparation of the manuscript.

**Competing Interests:** The authors have declared that no competing interests exist.

\* E-mail: awais\_mm@yahoo.com

## Introduction

The boundary layer flows in the presence of heat and mass transfer are important in the metallurgical processes involving the cooling of continuous strips. At present this topic has been studied extensively via different flow configurations and assumptions. Few representative investigations in this direction can be found in the refs. [1–5] In all these studies the research has been carried out for flows induced by moving surface in semi-infinite expanse of fluid. Very little is said about such flows in the bounded domains. Dinarvand and Rashidi [6] examined a reliable treatment of homotopy solution for two-dimensional viscous flow in a rectangular domain by considering two moving porous walls. Axisymmetric finite element solution of non-isothermal parallel-plate flow has been presented by Zhang and Olagunju [7]. Martinez et al. [8] discussed the viscous flow in a curved channel with flexible moving porous walls. Bifurcation of multimode flows of viscous fluid in a plane diverging channel is examined by Akulenko and Kumakshev [9]. Mahmood and Asif [10] studied generalized three-dimensional channel flow due to uniform stretching of plate. Recently, an incompressible moving boundary flows with the finite volume particle method has been examined by Nestor and Quinlan [11].

To our information, the MHD channel flow due to stretching surfaces with heat and mass transfer is not investigated yet in presence of thermal radiation. Needless to say that mass transfer is involved in the net movement of mass from one locality to another in the system and has abundant applications in chemical engineering. Specific applications include evaporation of water, the diffusion of chemical contamination, separation of chemicals in distillation procedure etc. For separation processes, thermodynamics determines the amount of separation, while mass transfer determines the rate at which the separation is possible. Further the heat transfer is a process that concerns with the exchange of thermal energy from one physical system to another. The

radiation effects are prominent in any transparent medium for instance solid or fluid, but may also even occur across vacuum in the form of electromagnetic rays. The purpose of current investigation is to examine the simultaneous effects of heat and mass transfer on the magnetohydrodynamic (MHD) three-dimensional channel flow of viscous fluid in the presence of thermal radiation. Section 2 includes the mathematical formulation and analysis with graphical results whereas section 3 includes the concluding remarks.

## Mathematical Formulation

Three-dimensional flow of an incompressible viscous fluid bounded by two infinite parallel plates (separated by distance  $h$ ) is considered here. The motion in fluid is due to equal and opposite forces along the  $x$ - and  $y$ -axes so that the plate is stretched in both directions keeping the origin fixed. The lower plate is a highly elastic membrane situated at  $z=0$  and the upper plate is uniformly subjected to constant injection in the channel fixed at  $z=h$ . A constant magnetic field of strength  $B_0$  is applied. In addition the heat and mass transfer effects in the presence of thermal radiations are also present. The flow is governed by the following expressions

$$\frac{\partial u}{\partial x} + \frac{\partial v}{\partial y} + \frac{\partial w}{\partial z} = 0, \quad (1)$$

$$u \frac{\partial u}{\partial x} + v \frac{\partial u}{\partial y} + w \frac{\partial u}{\partial z} = -\frac{1}{\rho} \frac{\partial p}{\partial x} + \nu \left( \frac{\partial^2 u}{\partial x^2} + \frac{\partial^2 u}{\partial y^2} + \frac{\partial^2 u}{\partial z^2} \right) - \frac{\sigma B_0^2}{\rho} u, \quad (2)$$

$$u \frac{\partial v}{\partial x} + v \frac{\partial v}{\partial y} + w \frac{\partial v}{\partial z} = -\frac{1}{\rho} \frac{\partial p}{\partial y} + \nu \left( \frac{\partial^2 v}{\partial x^2} + \frac{\partial^2 v}{\partial y^2} + \frac{\partial^2 v}{\partial z^2} \right) - \frac{\sigma B_0^2}{\rho} v, \quad (3)$$

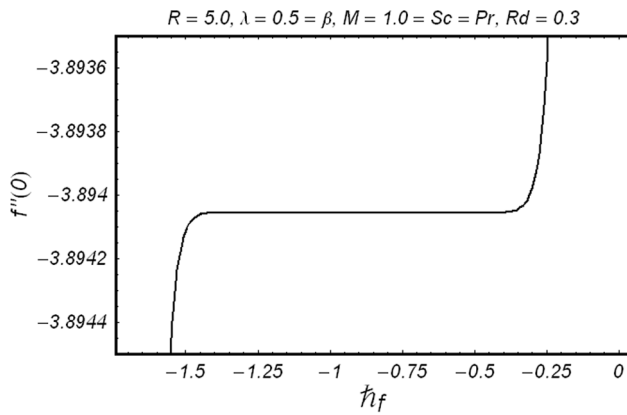


**Figure 1. h curve of  $f$  at the 15th order of approximation.**  
doi:10.1371/journal.pone.0086695.g001

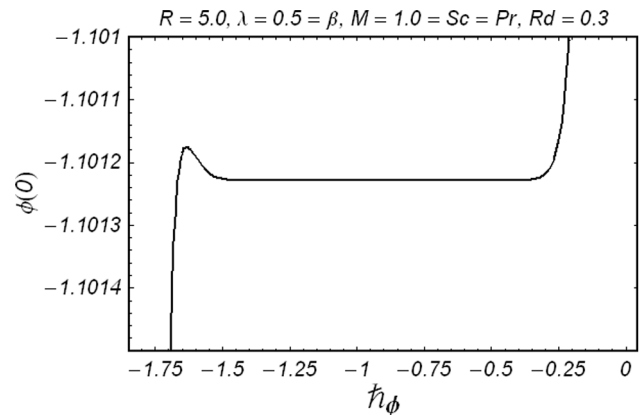


**Figure 3. h curve of  $\phi$  at the 15th order of approximation.**  
doi:10.1371/journal.pone.0086695.g003

$$u \frac{\partial w}{\partial x} + v \frac{\partial w}{\partial y} + w \frac{\partial w}{\partial z} = -\frac{1}{\rho} \frac{\partial p}{\partial z} + \nu \left( \frac{\partial^2 w}{\partial x^2} + \frac{\partial^2 w}{\partial y^2} + \frac{\partial^2 w}{\partial z^2} \right), \quad (4)$$

$$u \frac{\partial C}{\partial x} + v \frac{\partial C}{\partial y} + w \frac{\partial C}{\partial z} = D \frac{\partial^2 C}{\partial z^2}, \quad (5)$$

$$u \frac{\partial T}{\partial x} + v \frac{\partial T}{\partial y} + w \frac{\partial T}{\partial z} = \alpha_m \frac{\partial^2 T}{\partial z^2} + \frac{16\sigma^* T_0^3}{3k^* \rho c_p} \left( \frac{\partial^2 T}{\partial z^2} \right) \quad (6)$$

subject to the boundary conditions

$$u = u_w(x) = ax, \quad v = v_w(y) = by, \quad w = 0, \quad C = C_w, \quad T = T_w, \quad \text{at } z = 0,$$

$$u = 0, \quad v = 0, \quad w = -V_0, \quad C = C_n, \quad T = T_0 \quad \text{at } z = h. \quad (7)$$

In above equations  $u$ ,  $v$  and  $w$  are the velocities in the  $x$ ,  $y$  and  $z$  directions, respectively,  $V_0$  the constant injection velocity at upper wall,  $p$  the pressure,  $\nu$  the kinematic viscosity,  $\rho$  the density,  $\sigma$  the

electrical conductivity,  $\sigma^*$  the Stefan-Boltzman constant,  $k^*$  the Rosseland mean absorption coefficient,  $C$  the concentration of species,  $D$  the coefficients of diffusing species,  $T$  the temperature and  $\alpha_m$  the thermal diffusivity. The fluid phase temperature differences within the flow are sufficiently small so that  $T^4$  may be described as a linear function of temperature. Hence last term in Eq. (6) is obtained by expanding  $T^4$  in Taylor's series about the free-stream temperature  $T_0$  and neglecting higher order terms.

The boundary conditions for the present situation can be written in such a way that  $C_w$  denotes the concentration at the surface,  $C_0$  is the concentration far away from the sheet,  $T_w$  is the surface temperature and  $T_0$  is the temperature far away from the surface.

Using [10,17]

$$\eta = \frac{1}{h} z, \quad u = axf'(\eta), \quad v = ayg'(\eta), \quad w = -ah\{f(\eta) + g(\eta)\},$$

$$\theta(\eta) = \frac{T - T_0}{T_w - T_0}, \quad \phi(\eta) = \frac{C - C_0}{C_w - C_0} \quad (8)$$

the continuity equation is automatically satisfied and Eqs. (2)–(7) give

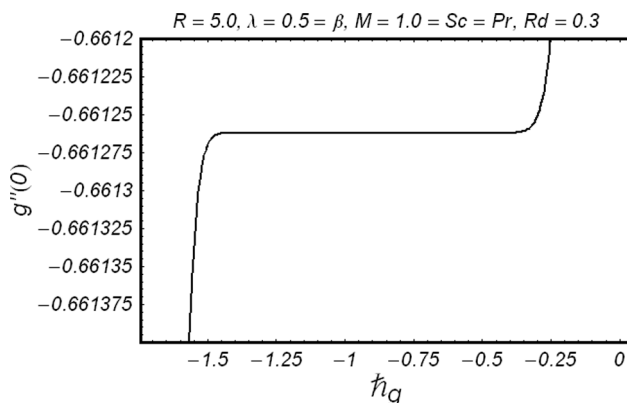


**Figure 2. h curve of  $g$  at the 15th order of approximation.**  
doi:10.1371/journal.pone.0086695.g002

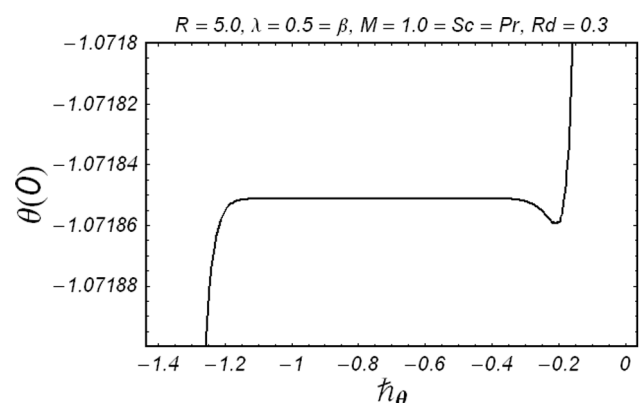


**Figure 4. h curve of  $\theta$  at the 15th order of approximation.**  
doi:10.1371/journal.pone.0086695.g004

**Table 1.** Convergence of the HAM solutions for different order of approximations when  $R = 5, \lambda = 0.25, \beta = 0.3, M = 1, Pr = 1 = Sc$  and  $Rd = 0.3$ .

order of approximation	$-f''(0)$	$-g''(0)$	$-\phi'(0)$	$-\theta'(0)$
1	3.902083333	0.6584325397	1.104166667	1.104166667
5	3.894097726	0.6612752030	1.101226749	1.072402632
10	3.894057150	0.6612623541	1.101228897	1.071850269
15	3.894057129	0.6612623520	1.101228896	1.071851257
20	3.894057129	0.6612623521	1.101228896	1.071851290
25	3.894057129	0.6612623521	1.101228896	1.071851290
30	3.894057129	0.6612623521	1.101228896	1.071851290
40	3.894057129	0.6612623521	1.101228896	1.071851290
50	3.894057129	0.6612623521	1.101228896	1.071851290
60	3.894057129	0.6612623521	1.101228896	1.071851290

doi:10.1371/journal.pone.0086695.t001

$$f^{iv} - \text{Re}(f'f'' - g'f'' - ff''' - gf''') - M^2f'' = 0, \tag{9}$$

$$g^{iv} - \text{Re}(g'g'' - f'g'' - fg''' - gg''') - M^2g'' = 0, \tag{10}$$

$$\phi'' + Sc[(f + g)\phi'] = 0, \tag{11}$$

$$(1 + \frac{4}{3}Rd)\theta'' + Pr[(f + g)\theta'] = 0, \tag{12}$$

$$f'(0) = 1, g'(0) = \beta, f + g = 0, \phi(0) = 1, \theta(0) = 1,$$

$$f'(1) = 0, g'(1) = 0, f + g = \lambda, \phi(1) = 0, \theta(1) = 0, \tag{13}$$

where  $\text{Re} = ah^2/\nu$  is the Reynolds number,  $\beta = b/a(a \neq 0)$  is the ratio of stretching coefficients,  $\lambda = V_0/ah$  is the dimensionless injection parameter,  $M^2 = \frac{\sigma B_0^2 h^2}{\rho\nu}$ ,  $Sc = ah^2/D$  is the Schmidt

number,  $Rd = \frac{4\sigma^* T_0^3}{k^*k}$  is the thermal radiation and  $Pr = ah^2/\alpha_m$  is the Prandtl number. Note that the constants  $a > 0$  and  $b > 0$ .

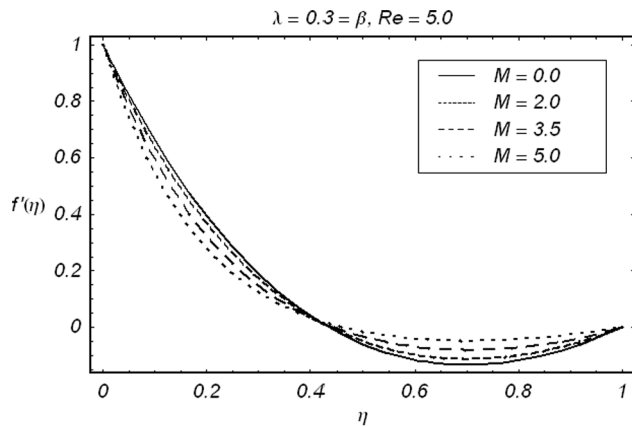
Now we solve Eqs. (8–11) along with the boundary conditions (12) by using homotopy analysis method. The details of homotopy analysis method are already included in our various published articles ([12–20]) and references there in) hence these are excluded here in order to save space. We choose auxiliary parameters  $h_f, h_g, h_\phi$  and  $h_\theta$  for the functions  $f, g, \phi$  and  $\theta$  respectively. These auxiliary parameters play a vital role in adjusting the convergence of the obtained series solutions. We have plotted  $h$ -curves in Figs. (1–4) to obtain the permissible values of these auxiliary parameters. It is found that range for admissible values of  $h_f, h_g, h_\phi$  and  $h_\theta$  are  $-1.5 \leq h_f, h_g, h_\phi \leq -0.3$  and  $-1.2 \leq h_\theta \leq 0.3$ . It is noticed that series solutions converge in the whole region of  $\eta$  ( $0 < \eta < 1$ ) for  $h_f, h_g, h_\phi$  and  $h_\theta = 1.0$ .

Table 1 signifies that how much order of approximations are required for a convergent solution. Obviously 15th order of approximations are sufficient for the analysis under consideration. In order to validate our results, we have given a comparative study of present results with the existing results. The results are in an excellent agreement (displayed in Table 2). Figs. (5–9) are displayed for the effects of different parameters on velocity, concentration and temperature fields. The effects of  $M$  on  $f'$  and  $g'$  have been depicted in the Figs. 5 and 6. It is seen from Fig. 5 that in view of an increase in Hartman number  $M$ , the velocity  $f'(\eta)$  decreases in the vicinity of stretching sheet ( $0 < \eta < 0.4$ ) whereas  $f'(\eta)$  increases away from the stretching sheet

**Table 2.** Comparison of values of  $-f''(0)$  and  $-g''(0)$  for viscous fluid ( $M = 0$ ) (refs.[10]) when  $\text{Re} = 5.0, \beta = 0.5$  and  $\lambda = 0.5$ .

Order of approximation	Present results		ref. [10] results	
	$-f''(0)$	$-g''(0)$	$-f''(0)$	$-g''(0)$
5	2.987025	0.5037159	2.98703	0.503716
10	2.990508	0.5037637	2.99051	0.503764
15	2.990524	0.5037629	2.99052	0.503763
20	2.990525	0.5037629	2.99053	0.503763
25	2.990525	0.5037629	2.99053	0.503763

doi:10.1371/journal.pone.0086695.t002



**Figure 5. Effect of  $M$  on the velocity component  $f'$ .**  
doi:10.1371/journal.pone.0086695.g005

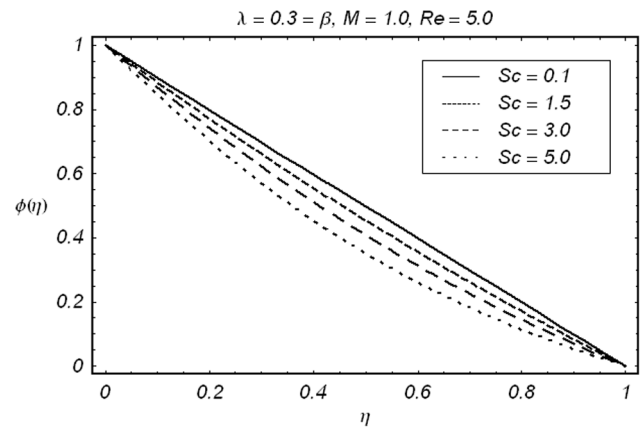


**Figure 7. Effect of  $Sc$  on  $\phi$ .**  
doi:10.1371/journal.pone.0086695.g007

( $0.4 < \eta < 1$ ). This is in accordance with the reason that magnetic field retards the fluid particles and slows down the motion in the vicinity of stretching sheets but obviously to satisfy mass conservation constraint a decrease in fluid velocity in the vicinity of stretching sheets is compensated by an increase in fluid velocity in the upper half of channel due to constant injection at the upper wall. This gives rise to a cross-over behavior which is obvious from Fig. 5. Variation of  $M$  on  $f'$  and  $g'$  are quite similar (see Fig. 6). The variation of  $Sc$  on the concentration field  $\phi$  is shown in Fig. 7. It is seen that concentration field  $\phi$  and concentration boundary layer are decreasing function of  $Sc$ . Since Schmidt number  $Sc$  is depending inversely on diffusion coefficient  $D$ . Hence an increase in  $Sc$  shows a decrease in diffusion  $D$ . This ultimately shows a decrease in concentration field  $\phi$ . Fig. 8 elucidates the effects of Prandtl number  $Pr$  on the temperature field  $\theta$ . Here temperature field  $\theta$  and thermal boundary layer thickness are decreasing function of  $Pr$ . This is because of the reason that larger Prandtl number corresponds to the weaker thermal diffusivity and thinner boundary layer. The influence of thermal radiation parameter  $Rd$  on  $\theta$  are given in Fig. 9. It is observed that thermal radiation causes a slight increase in temperature.

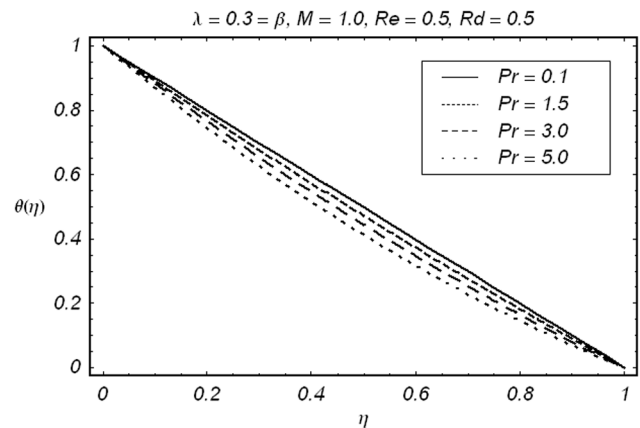


**Figure 8. Effect of  $Pr$  on  $\theta$ .**  
doi:10.1371/journal.pone.0086695.g008

**Concluding Remarks**

The present study describes the effects of heat and mass transfer on the magnetohydrodynamic (MHD) three-dimensional bound-

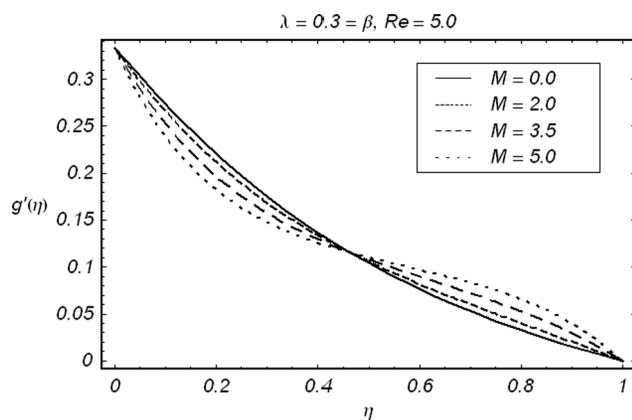


**Figure 6. Effect of  $M$  on the velocity component  $g'$ .**  
doi:10.1371/journal.pone.0086695.g006

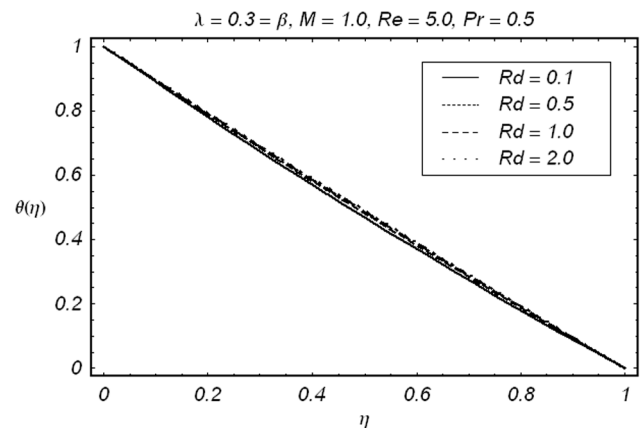


**Figure 9. Effect of  $Rd$  on  $\theta$ .**  
doi:10.1371/journal.pone.0086695.g009

ary layer flow of viscous fluid between two infinite parallel plates. The main points are summed up as follows:

- It is observed that magnetic field  $M$  retards the flow near the stretching boundary.
- Injection causes an increase in velocity to compensate the effects of magnetic field so that the mass conservation constraint is satisfied.
- Prandtl number  $Pr$  and radiation parameter  $Rd$  show opposite behavior on temperature field  $\theta$ .

## References

1. Sahoo B, Do Y (2010) Effects of slip on sheet-driven flow and heat transfer of a third grade fluid past a stretching sheet. *Int. Com. Heat Mass Transfer*, 37: 1064–1071.
2. Jamil M, Fetecau C, Imran M (2011) Unsteady helical flows of Oldroyd-B fluids. *Comm. Nonlinear Sci. Numer. Simulat.* 16: 1378–1386.
3. Wang S, Tan WC (2011) Stability analysis of solet-driven double-diffusive convection of Maxwell fluid in a porous medium. *Int. J. Heat Fluid Flow*, 32: 88–94.
4. Hayat T, Ali S, Awais M, Obaidat S (2013) Stagnation point flow of Burgers' fluid over a stretching surface. *Progress Comp. Fluid Dyn.* 13: 48–53.
5. Awais M, Alsaedi A, Hayat T (2013) Unsteady flow of Maxwell fluid with thermal-diffusion and diffusion-thermo effects. *Int. J. Numer. Meth. Heat Fluid Flow*, Inpress.
6. Dinarvand S, Rashidi MM (2010) A reliable treatment of a homotopy analysis method for two-dimensional viscous flow in a rectangular domain bounded by two moving porous walls. *Nonlinear Analysis: Real World Appl.* 11: 1502–1512.
7. Zhang S, Olagunju DO (2005) Axisymmetric finite element solution of non-isothermal parallel-plate flow. *Applied Math. Comp.*, 171: 1081–1094.
8. Martinez DM, Seo DJ, Jong J (2008) Viscous flow of a Newtonian fluid in a curved channel with flexible moving porous walls. *Chemical Engng. Sci.*, 63: 1882–1889.
9. Akulenko L, Kumakshev S (2008) Bifurcation of multimode flows of a viscous fluid in a plane diverging channel. *J. Appl. Math.Mech.* 72: 296–302.
10. Mehmood A, Ali A. (2007) Analytic homotopy solution of generalized three-dimensional channel flow due to uniform stretching of the plate. *Acta Mech Sin.* 23: 503–510.
11. Nestor RM, Quinlan NJ (2010) Incompressible moving boundary flows with the finite volume particle method. *Comp. Methods Appl. Mech. Eng.*, 199: 2249–2260.
12. Liao SJ (2004) On the homotopy analysis method for nonlinear problems. *Appl. Math. Comp.* 147: 499–513.
13. Abbasbandy S, Shirzadi A (2011) A new application of the homotopy analysis method: Solving the Sturm–Liouville problems. *Comm. Nonlinear Sci. Numer. Simulat.* 16: 112–126.
14. Abbasbandy S, Hayat T (2011) On series solution for unsteady boundary layer equations in a special third grade fluid, *Comm. Nonlinear Sci. Numer. Simulat.* 16: 3140–3146.
15. Bataineh AS, Noorani MSM, Hashim I (2008) Approximate analytical solutions of systems of PDEs by homotopy analysis method. *Comp. Math. Appl.* 55: 2913–2923.
16. Bataineh AS, Noorani MSM, Hashim I (2009). On a new reliable modification of homotopy analysis method. *Comm. Nonlinear Sci. Numer. Simulat.* 14: 409–423.
17. Hayat T, Awais M, Obaidat S (2012) 3-D flow of a Jeffery fluid in a channel of lower stretching wall. *Euro. Phys. J. Plus*, 127: 128–138.
18. Hayat T, Awais M, Asghar S, Obaidat S (2012) Unsteady flow of third grade fluid with Soret and Dufour effects. *ASME, J of Heat Transfer*, 134: 062001.
19. Rashidi MM, Pour SAM, Hayat T, Obaidat S (2012) Analytic approximate solutions for steady flow over a rotating disk in porous medium with heat transfer by homotopy analysis method. *Computers & Fluids*, 54: 1–9.
20. Rashidi MM, Pour SAM, Abbasbandy S (2011) Analytic approximate solutions for heat transfer of a micropolar fluid through a porous medium with radiation. *Comm. Nonlinear Sci. Numer. Simulat.*, 16: 1874–1889.

## Author Contributions

Conceived and designed the experiments: MA AS. Analyzed the data: MA TH AS. Contributed reagents/materials/analysis tools: MA. Wrote the paper: MA. Provided financial support: AA.